POSITRON ANNIHILATION STUDY OF VACANCY DYNAMICS AFTER THE SOLUTION TREATMENT OF Al-Zn-Mg ALLOYS

Rafael FERRAGUT[*], Alberto SOMOZA[*] and Alfredo DUPASQUIER[**]

[*] IFIMAT, Universidad Nacional del Centro de la Provincia de Buenos Aires,
Pinto 399, 7000 Tandil, Argentina and
Comisión de Investigaciones Científicas de la Provincia de Buenos Aires, Argentina
[**] Istituto Nazionale di Fisica della Materia
Dipartimento di Fisica, Politecnico di Milano, Piazza L. da Vinci, 32
I-20133 Milano, Italia

ABSTRACT: Positron annihilation lifetime spectroscopy and Vickers microhardness were used to follow microstructural changes induced by multiple-step aging thermal treatments on different commercial age-hardening Al-Zn-Mg alloys (7005 and 7012). From the positron lifetime and microhardness data it was possible to obtain information on the time evolution of formation, dissolution and recuperation of GP zones and formation of semicoherent precipitates η'. It was also possible to derive activation energies for the solute-vacancy complexes migration. It was observed a strong dependence on the composition of the alloys, to be ascribed to the Mg content and to the quaternary additions (Cu, Mn). Direct information about sizes and morphologies of GP zones and η' particles was obtained by high-resolution and conventional-resolution transmission electron microscopy.

Keywords: *Al-based age-hardenable alloys, vacancies, precipitates, Guinier-Preston zones, positron annihilation lifetime spectroscopy*

1. INTRODUCTION

It is well known from experiments that clustering and decomposition processes in supersaturated alloys are accompanied by characteristic changes in the physical properties. This is widely used in material science and technology in order to control the hardening of aluminum alloys. Aging normally takes place through a sequence of stages, during which metastable phases are initially formed and then disappear or are transformed into more complex but more stable phases. For Al-Zn-Mg alloys, the aging sequence is : αSSS (supersaturated solid-solution) → spherical Guinier Preston zones → ordered GP zones → transition phase η' → stable precipitates η [1,2]. The formation of GP zones already occurs at (or near to) room temperature; at higher temperatures, the GP zones disappear, but their initial presence favors a more homogeneous nucleation of semicoherent precipitates with composition $Mg(Zn,Al)_2$ (η' particles). In turn, the presence of the η' particles has a strong influence on the nucleation of the η phase, which is fully incoherent with the matrix. The sequence of stages in the decomposition process depends on the composition of the alloy, on the quenching conditions, on the aging temperatures, etc. (for a review see [1,2]).

In the last twenty years positron annihilation spectroscopy (PAS) has been successfully used to study precipitation kinetics in prepared Al-based age-hardenable alloys. More specifically, positron lifetime and Doppler broadening measurements have been applied to study precipitation phenomena in prepared Al-Zn and Al-Zn-Mg alloys as well as in commercial Al-Zn-Mg systems (see details in [3-5]. For staying on a firm ground, examples based on recent experience with commercial alloys of the 70XX series are given in [6,7]. In these studies, we have tried to obtain a detailed physical picture of the evolution of the alloy by adopting a kinetic approach, i.e. by taking measurements at various aging times.

In the present investigation we have combined Positron Annihilation Lifetime Spectroscopy (PALS) with Vickers microhardness measurements in order to characterize various stages of age hardening of Al-Zn-Mg commercial systems. We have obtained information on: a) the microstructural changes (formation, dissolution, reconstruction and growth of GP zones and of η' precipitates) occurring as a consequence of pre-aging and a further aging treatment; b) the activation energies of the above processes; c) the effect of the main secondary alloying element (quaternary additive). Some PAS and hardness results will be discussed and compared with a preliminary direct information about structure, morphology and orientation relationships of precipitates obtained by high resolution and by conventional resolution transmission electron microscopy (HRTEM and CRTEM).

On the other hand, the present work is an attempt to specify the type of information that can be expected from PAS in the study of decomposition processes of age-hardenable alloys. It will be discussed below what positron experiments on multiple-step aging heat treated specimens can tell us regarding the effects of the different aging procedures.

2. EXPERIMENTAL

For the present study, we have chosen two alloys of the 70XX series, namely 7005 and 7012, which have about the same Zn-to-Mg ratio, but with a different quaternary additive (Mn in alloy 7005 and Cu in alloy 7012). In detail, the compositions of the two systems is: i) **alloy 7005**: Al-4.6wt.%Zn-1.4wt.%Mg-0.5wt.%Mn, also containing (in wt.%) 0.1 Cr, 0.1 Zr, 0.03 Ti, Fe < 0.4, Si < 0.35 and Cu < 0.1, ii) **alloy 7012**: Al-6.0wt.%Zn-2.0wt.%Mg-1.0wt.%Cu, also containing (in wt.%) 0.12 Zr, 0.10 Mn, 0.06 Ti, Fe < 0.25, Si < 0.15 and Cr < 0.04.

Specimens in the form of discs of 1.5 mm thickness were cut from a rod of 10 mm diameter by a low speed diamond saw. Solution treatments were carried out in an air circulating furnace at 475 °C for 2 h and then the samples were quenched in water at room temperature (RT ≈ 20 °C). The first step of aging (pre-aging) was performed at RT or 45 °C or 70 °C up to about 5 days. Thereafter, the second step of aging was performed in a glycerine bath at 150 °C for different times up to 2000 min. At the end of each thermal treatment, the samples were given a metallographic polishing with diamond paste up to 1 μm followed by a dilute Keller etching.

The lifetime spectrometer was a fast-fast timing coincidence system with a time resolution (FWHM) of 255 ps. A 20 μCi source of $^{22}NaCl$ deposited on a thin Kapton foil (1.1 mg/cm^2) was sandwiched between two identical alloy specimens. The lifetime spectra were analyzed using the POSITRONFIT program [8]. After subtracting the source component (τ_s = 382 ps, I_s = 10.5 %), the spectra were satisfactorily analyzed with a single lifetime component. The total number of counts in each spectrum was about 10^6, accumulated in a time interval of 14400 s. Lifetime spectra and hardness data were always taken at room temperature.

Vickers microhardness measurements were performed after each positron lifetime measurement by using a load of 100 g; the diagonal of the square explored by the indentor was about 40 μm.

Specimens for transmission electron microscopy were prepared by mechanical grinding and twin-jet electropolishing in a solution of 1/3 nitric-acid in methanol at –35° C.

3. RESULTS AND DISCUSSION

Two-step aging treatments are a standard procedure used for improving the mechanical characteristics of age-hardenable alloys after the initial homogenization treatment. The experimental data of Fig. 1 obtained on samples of alloy 7005 represent these different stages. The first one (*pre-aging*), where positron lifetime τ and Vickers microhardness H_V are shown as a function of aging time, is an isothermal treatment at RT or at another temperature sufficiently low to avoid the nucleation of incoherent particles (for sake of simplicity , we have omitted in Fig. 1 the evolution of positron lifetime and hardness for 45 °C and 70 °C). *Artificial aging* is the second step of the

classical two-step aging treatments used for treating age-hardenable alloys. In Fig. 1 the evolution of the 7005 alloy (a similar behavior was observed in the 7012 alloy, see Fig. 2) during artificial aging at 150 °C after a pre-aging of five days at RT is plotted as a function of the aging time. The time scale chosen in these figures is $t^{1/3}$; this is a convenient choice for representing a structural evolution occurring in a coalescence regime, as implied by the Lifshitz-Slyozov-Wagner coarsening theory (see [5] for a discussion of the validity of this theory as a description of the coarsening of GP zones).

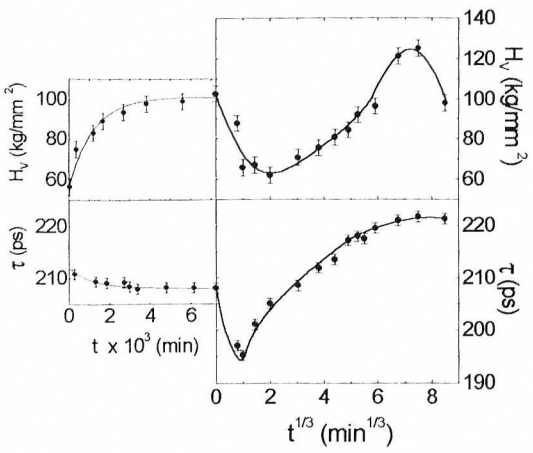

Fig. 1: Evolution of the positron lifetime τ and the Vickers hardness H_V of the 7005 alloy during pre-aging at RT and artificial aging at 150 °C (see text).

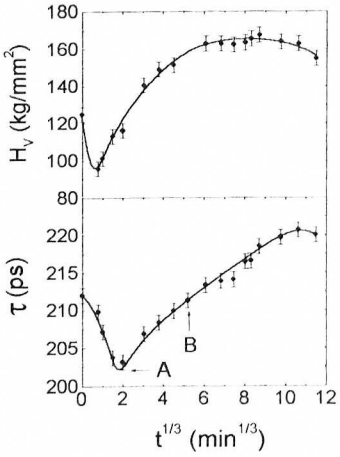

Fig. 2: Evolution of the positron lifetime and microhardness of the 7012 alloy during artificial aging at 150 °C (solid line is a visual guide).

The experimental results mentioned mentioned above, can be qualitatively interpreted as follows: i) *During pre-aging*, the experimental data of Fig. 1 corresponding to alloy 7005 (a similar behavior for different temperatures was observed in the 7012 alloy [8]) show that τ slightly decreases and H_V strongly increases; a detailed discussion about this behavior is given below; ii) *After pre-aging*, from the positron lifetime τ_{GP} ~210 ps (which is too long to be attributed to annihilation in bulk τ_{GP} ~165 ps), we can establish that the GP zones have already reached a concentration sufficient to trap all positrons. Inside the GP zones, the positrons are localized in stable vacancies associated with Mg atoms [4-7] (ii) *During artificial aging*, the initial effect of this heat treatment is a strong decrease of the hardness and of the positron lifetime. The decrease is followed by an increasing stage that eventually brings both parameters to a new maximum above the initial value. In previous works [6,7], the increase of H_V and τ was assigned to the fact that after an incubation period dominated by the coarsening of the GP zones (the biggest GP zones absorb the solute coming from the dissolution of the small ones), the residual GP zones, too big to remain stable, are transformed into η' particles. As this transformation proceeds, an increasing fraction of positrons gets trapped in the misfit region at the incoherent interface between precipitates and the matrix. For a sufficiently long aging time, trapping at the surface of η' precipitates becomes dominant and the lifetime reaches a new plateau. However, the transformation $GP \rightarrow \eta'$ does not explain the important initial decrease of τ and H_V observed in Figs. 1 and 2. A similar temporary softening was already observed in different age-hardenable Al-based alloys and was interpreted as reversion [9,10]; the PAS results confirm this interpretation with direct evidence of reduced trapping in GP zones. This phenomenon is only temporary, and can be observed only if the PAS measurements are performed shortly after the interruption of the heat treatment; when the data are taken several weeks later, as in the case of the previous works on alloy 7012 [5], the evolution of the sequence of points appears strictly monotonic

and is entirely determined by the transformation $GP \rightarrow \eta'$. Clearly, the effect has nothing to do with the η' phase, but indicates that trapping in GP zones falls below saturation.

In order to obtain a complementary microstructural evidence of some of the processes described above, we have used TEM techniques.The micrographs of Fig. 3 (a) and (b) obtained on samples of alloy 7012 correspond to the experimental situation of point A of the Fig. 2, in which the positron lifetime reaches the minimum value during isothermal artificial aging at 150 °C. In the CRTEM micrograph of Fig. 3 (a) it is possible to distinguish particles with different contrast, i.e. *i)* thin plates aligned into two orientations forming an angle of 71° between them, having between 6 nm and 8 nm as a larger size, these particles are found on {111}Al planes; *ii)* circular-like particles with sizes about 8 nm; and *iii)* a background formed by spherical particles (GP zones) smaller than the above mentioned particles. Fig. 3 (b) is a HRTEM micrograph of the same microstructure shown in Fig. 3 (a), in this case it is possible to obtain, which more precision, the size of the platelets *i)* which have 7.4 nm length and 1.7 nm width. Figure 3 (a) and (b) also show that the non-dissolved GP zones coexist with small quantity of incipient η' precipitates. Fig. 3 (c) shows a CRTEM micrograph for the artificial aging stage indicated by the point B of Fig. 2, for which the positron lifetime recover the positron lifetime corresponding to the after pre-aging situation. In this case, particles of type *i)* or *ii)* having sizes between 8.5 nm and 15 nm, respectively, are observed. In agreement with published results [11-13], we have found that in the observed samples appear disc-shaped η' precipitates; we have also observed that the faces of the particles are parallel to two types of {111}Al planes perpendicular to the micrograph plane (parallel to zone axis [110]).

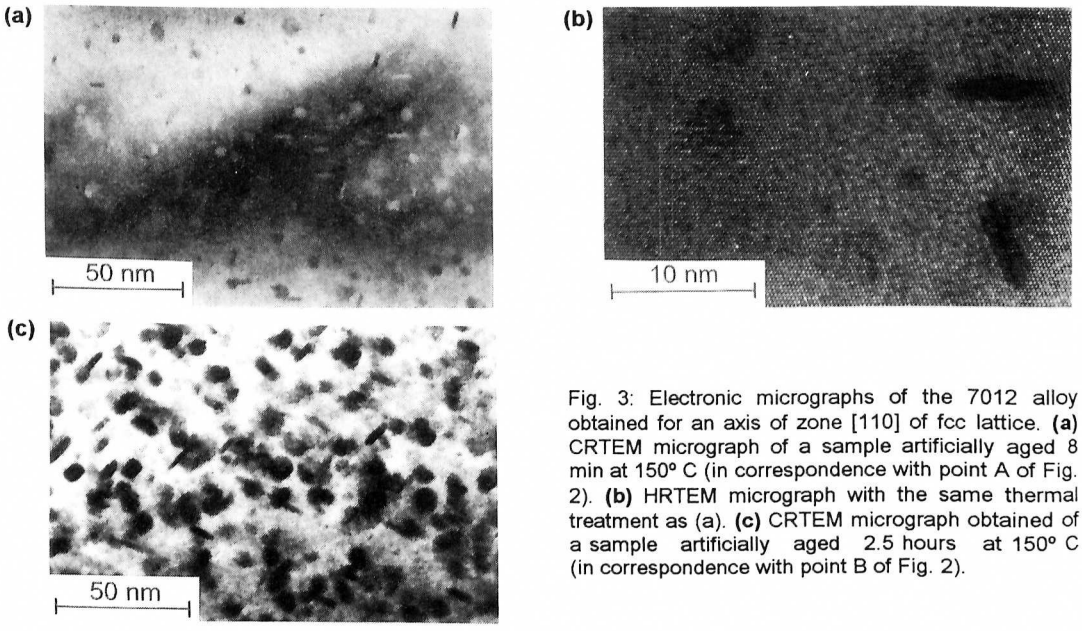

Fig. 3: Electronic micrographs of the 7012 alloy obtained for an axis of zone [110] of fcc lattice. **(a)** CRTEM micrograph of a sample artificially aged 8 min at 150° C (in correspondence with point A of Fig. 2). **(b)** HRTEM micrograph with the same thermal treatment as (a). **(c)** CRTEM micrograph obtained of a sample artificially aged 2.5 hours at 150° C (in correspondence with point B of Fig. 2).

If the artificial aging is interrupted by rapid cooling at RT during the partial reversion stage (in the 7005 alloy after an aging of 1 min at 150 °C, τ has reached its minimum), τ gradually recovers its initial value corresponding to the end of the RT pre-aging (similar behavior is observed in the 7012 alloy [7,8]). Besides, the soft material also recovers the initial hardness values for both alloys. With a short aging time, the dissolution of the smallest GP zones is well advanced or even complete; the coarsening of GP zones and the formation of η' particles have not taken place yet or are still at a very initial stage. With the interruption of the aging treatment, coarsening and transformation do not occur and the excess solute, initially present in the matrix, is redistributed in a dissemination of small GP zones.

Experimental information like that one shown in Fig. 4, corresponding to positron lifetime data, give quantitative information about the time law governing the possible reconstruction of the GP zones or the growth of η' particles in the 7005 alloy for different moderate temperatures, and show that this process occurs at all temperatures explored in the present work. The difference among the saturation values of the positron lifetimes at 70 °C and those obtained at lower temperatures (up to 45 °C) seems to indicate that the microstructural transformations are not exactly the same; we have previously mentioned that at 70 °C , together with the recuperation of GP zones, an incipient formation of η' particles might take place [7].

In order to obtain a physical characterization of the thermal activation process of reconstruction, the experimental data were fitted with curves corresponding to exponential time laws of the form

$$F = F_f - (F_f - F_i)\, e^{-t/t_c} \qquad (1)$$

where F represents either H_V or τ parameters, subindexes f and i represent the final and initial values of the parameters mentioned above and t_c is a characteristic time. In previous works we have found that it is possible to fit microhardness data (not included in this paper) and positron lifetimes for each alloy with almost identical values of t_c, in some way, it demonstrates that the two different parameters reveal the same microstructural changes [6,7]. By using the expression derived by Panseri and Federighi for the *Jump Model* [14]

$$t_c = t_0 \exp(E / k_B T) \qquad (2)$$

t_0 being a constant and k_B the Boltzmann constant, it is possible to obtain from the data taken at different temperatures the activation energy E relative to the microstructural transformations that occur during recovery through the transport of solute atoms or complexes in solid solution.

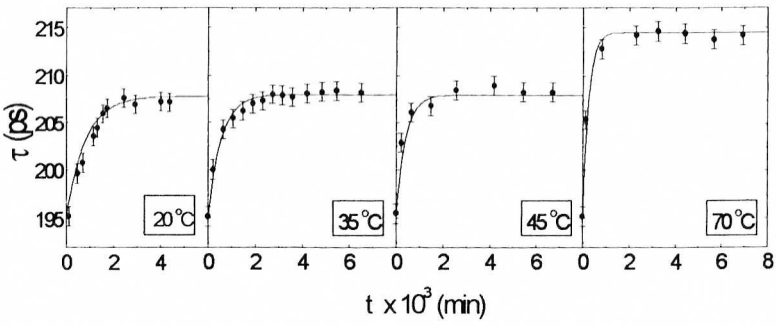

Fig. 4: Evolution of positron lifetime in alloy 7005 during aging at 20 °C (RT), 35 °C, 45 °C and 70 °C, after 1 min aging at 150 °C (corresponding to the minimum of the curve in Fig. 1). The solid lines represent a fitting of the experimental data with the exponential functions of the form of Eq.(1).

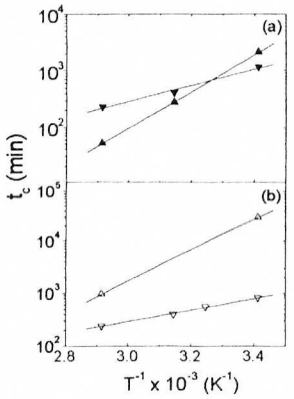

Fig. 5: Arrhenius plot for the characteristic time t_C obtained by fitting the pre-aging evolution (plot **a**) and the recovery process (plot **b**) for 7005 (▼▽) and 7012 alloys (▲△).

The opposite trends of τ and H_V observed during pre-aging, as shown in the left side of Fig. 1, contrasts with the apparent positive correlation observed during artificial aging, as shown in Figs. 1 (right side), 2 and 4. This effect certainly comes from the formation of GP zones at the expense of the vacancy clusters and of the vacancy-solute pairs that survive in the alloy at the end of the homogenization treatment. Thus, the modest decrease of τ would be the result of a slight unbalance of two opposite contributions: reduction of trapping at vacancy clusters and at the isolated vacancy-

solute pairs, partially compensated by the increase of trapping in GP zones. Microhardness, on the contrary, is insensitive to point-like defects; thus, its increase comes only from the formation of GP zones.

By fitting the pre-aging experimental data of Fig. 1 (we have also obtained similar behaviors for 7005 and 7012 alloys at 20 °C, 45 °C and 70 °C) with the exponential functions of the forms expressed by eq. (1) (see solid curves) characteristic times can be also obtained leading to the activation energies corresponding to the transformation phenomena during this aging step.

In Fig. 5 Arrhenius plots for the critical time obtained for the microstructural evolution at different temperatures during pre-aging and during the recovery process after partial aging for both alloys are shown, we also include results previously obtained for both processes from [6,7]. The corresponding activation energies obtained from the best-fit of the experimental data seems to be independent on the heat treatment. On the contrary, they are strongly dependent on the chemical composition of the alloy (the mean values are $E = 0.62 \pm 0.05$ eV for the 7012 alloy and $E = 0.25 \pm 0.05$ eV for the 7005 alloy). The different values of the activation energy indicate that the diffusing species that limit the nucleation and the formation of the GP II zones are not the same for the two alloys. Identification of these species may be attempted on the basis of comparison with the following data reported in the literature for prepared Al-Zn and Al-Zn-Mg alloys:

a) migration of the Zn-vacancy complex (ZnV): 0.42 eV in Al-Zn [15] and in Al-Zn-Mg [15] with an atomic concentration ratio C_{Mg}/C_{Zn} below 0.38;

b) migration of the Zn_2-vacancy complex (Zn_2V): 0.21 eV for Al-Zn-Mg [16] with an atomic concentration ratio C_{Mg}/C_{Zn} between 0.38 and 1.7) (the atomic concentration ratio is 0.82 for alloy 7005 and 0.90 for alloy 7012);

c) migration of the Mg-vacancy complex (MgV): 0.60 eV (see [1] and referenced therein).

These data suggest Zn_2V as the dominant diffusing species for alloy 7005 and MgV for the alloy 7012. The reason for the dominance of one diffusing species in one alloy and another species in the other alloy must lie in the respective chemical compositions. Possible microscopic mechanisms that justify the effect of the composition on the migration of solutes were discussed in [16]. Alloys 7005 and 7012 have almost the same magnesium-to-zinc ratio; the main points of difference are: a) the absolute value of the Mg content (1.4 wt. % in alloy 7005, 2 wt. % in alloy 7012), a factor that seems to influence rather strongly the diffusion processes in special cases [15,17]; b) the quaternary element (Mn in alloy 7005, Cu in alloy 7012). It is known that additions of Cu to Al-Zn-Mg alloys favour the formation of GP II zones and delay the rate of η' precipitation, while Mn acts in the opposite way [11]. The microscopic action of Cu could be the capture of a number of vacancies, thereby reducing the quantity available for the formation of movable complexes with the main solute elements. On raising the Mg content, the residual vacancies should be mostly captured by Mg atoms, thus reducing the concentration of the Zn_2V complex.

REFERENCES

[1] H Löffler,Y. Kovacs and J. Lendvai: J. Mat. Sci., **18**(1983), 2215.
[2] H. Löffler (Ed.) *"Structure and Structure Development of Al-Zn Alloys"*, (Akademie Verlag, Berlin, 1995)
[3] G. Dlubek: Mater. Sci. Forum, **13-14**(1987), 15.
[4] A. Somoza: Mater. Sci. Forum, **255-257**(1997), 86.
[5] S. Abis, M. Biasini, A. Dupasquier, P. Sferlazzo. and A. Somoza: J. Phys.:Condens. Matter, **1**(1989), 3679.
[6] R. Ferragut, A. Somoza and A. Dupasquier: J. Phys. Cond. Matter, **8**(1996), 8945.
[7] R. Ferragut, A. Somoza and A. Dupasquier: J. Phys. Cond. Matter, **10**(1998), in press.
[8] P. Kirkegaard P., N.J Pedersen and M. Eldrup M *PATFIT-88 Program*, (Risø National Laboratory M-2740, Roskilde, Denmark, 1989).
[9] K.S. Kumar, S.A. Brown. and J.R. Pickens: Acta mater., **44**(1996), 1899.
[10] F.W. Gayle, F.H. Heubaum. and J.R. Pickens: Scripta metall. mater., **24**(1990), 79.
[11] A. Kelly and R. B. Nicholson: Prog. Mat. Sci., **10**(1963), 216.
[12] A. Deschamps, Y. Bréchet, P. Guyot and F. Livet: Z. Metallkd., **88**(1997), 601

[13] J. K. Park and A. J. Ardell: Metall. Trans. A, **14**(1983), 1957.
[14] C. Panseri and T. Federighi: Acta metall., **11**(1963), 575.
[15] G. Jürgens, M. Kempe and H. Löffler: phys. stat. sol. (a), **21**(1974), K39.
[16] G. Jürgens, M. Kempe and H. Löffler: phys. stat. sol. (a), **25**(1974), K73.
[17] See [2], p.352.